Scientia Iranica D (2017) 24(6), 3257–3267

Sharif University of Technology
Scientia Iranica
Transactions D: Computer Science & Engineering and Electrical Engineering
www.scientiairanica.com

Poincaré section-based biomarkers of hemispheric asymmetry applied to autism spectrum disorder

Gh. Sadeghi Bajestani[a], A. Sheikhani[a], M.R. Hashemi Golpayegani[b,*], F. Ashrafzadeh[c] and P. Hebrani[d]

a. *Department of Biomedical Engineering, Science and Research Branch, Islamic Azad University, Hesarak, Tehran, P.O. Box 1477893855, Iran.*
b. *Department of Biomedical Engineering, Amirkabir University of Technology, 424 Hafez Ave., Tehran, 15875-4413, Iran.*
c. *Paediatrics Neurology Division, Ghaem Hospital, Mashhad University of Medical Sciences, Mashhad, Iran.*
d. *Department of Paediatrics, Dr. Sheikh Paediatric Hospital, Mashhad University of Medical Sciences, Mashhad, Iran.*

Received 20 February 2016; received in revised form 26 June 2016; accepted 18 July 2016

KEYWORDS
Autism spectrum disorder;
Poincaré section;
Hemispheric asymmetry;
Information.

Abstract. Asymmetry and symmetry coexist in natural and human processes, and the interaction of asymmetric action (recursion) and symmetric opposition (sinusoidal waves) is instrumental in generating creative features. Autism Spectrum Disorder (ASD) is a disorder in which asymmetry and functionality of brain hemispheres are affected. In this study, difference in brain asymmetry in ASD and normal children and the effect of voice on asymmetry are being investigated. Due to abnormal cortical voice processing in ASD, data recording is done in two situations: animation with audio (V-A) for 5 minutes and watching the animation with muted audio band (VwA). Two Indexes Divergence (D) and number of Poincaré section points further from threshold (HD) as new biomarkers are being extracted. Hemispheric asymmetry in ASD children does not follow norm patterns, and H and HD indexes confirm a disorder in hemisphere's functionality in all statistical tests which can be globally unveiled with Poincaré section and extracted information. Two remarkable features of the presented method are: data recording protocol specialized for ASD children and new practical time-series analysis for detecting episodic patterns (complexes) as hallmark of ASD dynamic and arrangement as an empirical measure of nonrandom complexity. The presented method could detect these complexes.

1. Introduction

The term symmetry originally means a sense of harmonious, aesthetically pleasing proportionality that embodies beauty. Soon, the term symmetry acquired a more precise meaning of mathematical balance such as when one shape becomes exactly like another if it is flipped ("mirror" symmetry), slid, or turned. Over the time, symmetry came to be defined when this internal identity could be demonstrated according to the rules of a formal system [1,2]. A mathematical object is symmetric with respect to a given mathematical operation if this operation preserves some properties of the object, when applied to the object. The most unique aspect in human brain organization is asymmetry based on which brain hemispheres nearly have separate functions and structures. Brain hemispheric asymmetry might vary regarding different reasons [3].

*. *Corresponding author. Tel.: +98 21 64542370;*
E-mail addresses: g.sadeghi@imamreza.ac.ir (Gh. Sadeghi Bajestani); sheikhaniali@yahoo.com (A. Sheikhani); mrhashemigolpayegani@aut.ac.ir (M.R. Hashemi Golpayegani); AshrafzadehF@mums.ac.ir (F. Ashrafzadeh); phebrani@yahoo.com. (P. Hebrani)

doi: 10.24200/sci.2017.4356

Autism is a disorder which might affect brain functions. Autism is a neurodevelopmental disorder recognizable with flaws in social communications and interactions and repetitive behavioral patterns, interests, and activities. The essential clinical features of autism spectrum disorder in Diagnostic and *Statistical Manual of Mental Disorders (DSM-5)* are: persistent impairment specific to reciprocal social communication and social interaction (Criterion A); restricted, repetitive patterns of behavior, interests, or activities (Criterion B). These symptoms are present as of early childhood and limit or impair our everyday functioning (Criteria C and D) [4]. These clinical presentations are mostly detected in childhood; other behaviors are frequently found in Autism Spectrum Disorders (ASDs) such as neophobia, enhanced anxiety, abnormal pain sensitivity and eye blink conditioning, disturbed sleep patterns, seizures, and deficits in sensorimotor gating [5,6]. Recent epidemiologic studies have estimated the ASD prevalence of 1 out of 68 children [7].

Numerous studies have shown that brain hemispheric asymmetry in ASD with regard to normal people is entirely different. In this field, widespread studies have been carried out using EEG in which different tools are applied to investigate asymmetry [8-14], and different indexes are introduced as biological indexes, some of which are mentioned in Table 1.

Although it is precisely mentioned in some articles that there has not been detected a biological index for ASD disorder yet [15], it seems that non-globalism in the results is abridged in non-globalism in tools. In this research, another tool, named "*Poincaré section*", is implemented to extract biomarkers with the aim of unveiling disorder in brain asymmetry of ASD cases, in which globalism, holism, and cybernetic approach are the main features. In the forthcoming sections, the results and conclusions are analyzed and preceded by introduction of the essence of Poincaré section and its implementation in addition to signal recording protocol.

2. Definitions

Newton and Leibniz are the origin of dynamical system theory and *Poincaré* is the first person who discover a chaotic deterministic system. Newton and Leibniz developed calculus to study celestial mechanics–the motion of the stars and planets and *Poincaré* solved, three-body problem. At the heart of these theory are differential equations that express the temporal dynamics of a system's state variables according to the physical laws governing the system. Some definitions are as below

- An *nth-order autonomous continuous-time dynamical system* is defined by the state equation:

$$\dot{x} = f(x), \qquad x(t_0) = x_0, \tag{1}$$

where $\dot{x} := \frac{dx}{dt}$, $x(t) \in \mathbb{R}^n$ is the state at time t, and $f : \mathbb{R}^n \to \mathbb{R}^n$ is called the *vector field*. Since the vector field does not depend on time, the initial time may always be taken as $t_0 = 0$;

- An *nth-order non-autonomous continuous-time dynamical system* is defined by the state equation:

$$\dot{x} = f(x, t), \qquad x(t_0) = x_0. \tag{2}$$

For non-autonomous systems, the vector field depends on time and, unlike the autonomous case, the initial time cannot, in general, be set to 0. The solution to Eq. (2) passing through x_0 at time t_o is denoted by $\varphi_t(x_0, y_0)$. Dynamical system (2) is linear if vector field, $f(x, t)$, is linear with respect to x [16];

- An nth-order time-periodic non-autonomous system with period T can always be converted into an $(n + l)$th-order autonomous system by appending an extra state $\theta := 2\pi t/T$. The autonomous system is given by:

$$\dot{x} = f(x, \theta T/2\pi) \qquad x(t_0) = x_0,$$

$$\dot{\theta} = 2\pi/T \qquad \theta(t_0) = 2\pi t_0/T. \tag{3}$$

Since f is time periodic with period T, System (3) is periodic in θ with period 2π. Hence, the planes,

Table 1. Important indexes used as biomarker in ASD.

Biomarker	Ref.
EEG complexity as a biomarker (multiscale entropy).	[47,48]
Higuchi's fractal dimension and Katz's fractal dimension.	[49]
Time and frequency domain and principal component analysis.	[48]
Spectral features.	[50-52]
EEG coherence for six frequency bands (delta, theta, alpha, sigma, beta, and total spectrum).	[53,54]
Power spectral.	[55-57]
EEG power and coherence.	[58,59]
Wavelet decomposition.	[60]
Mu rhythm investigation.	[18,19,61]

i.e. $\theta = 0$ and $= 2\pi$, may be identified and the state space is transformed from Euclidean space $\mathbb{R}^{n+1}$ to cylindrical space $\mathbb{R}^n \times S^1$ where $S^1 := [0, 2\pi)$ denotes the circle.

The solution to Eq. (3) in the cylindrical state space is:

$$\begin{bmatrix} x(t) \\ \theta(t) \end{bmatrix} = \begin{bmatrix} \phi_t(x_0, t_0) \\ 2\pi t/T \text{mod} 2\pi \end{bmatrix}, \quad (4)$$

where the modulo function restricts $0 \leq \theta < 2\pi$. Using this transformation, the theory of autonomous systems can be applied to time-periodic non-autonomous systems [16];

- A classical technique for analyzing dynamical systems is due to the issue of Poincaré. It replaces the flow of an nth-order continuous-time system with an $(n-l)$th-order discrete-time system called the Poincaré map. The definition of the Poincaré map ensures that its limit sets correspond to those of the underlying flow. The Poincaré map's usefulness lies in the reduction of order and the fact that it bridges the gap between continuous- and discrete-time systems.

The Poincaré map of non-autonomous systems: Recall that a time-periodic nth-order non-autonomous system with minimum period T can be transformed into an $(n+l)$th-order autonomous system in cylindrical state space $\mathbb{R}^n \times S^1$ via eq. (3).

Consider that n-dimensional hyper plane $\sum \in \mathbb{R}^n \times S^1$ is defined by:

$$\sum := \{(x, \theta) \in \mathbb{R}^n \times S^1 : \theta = \theta_0\}. \quad (5)$$

In every T second, Trajectory (4) intersects S (Figure 1). The resulting map $P_N : \sum \to \sum(\mathbb{R}^n ??? \mathbb{R}^n)$ is defined by $P_N(x) := \emptyset_{t_0+T}(x, t_0)$.

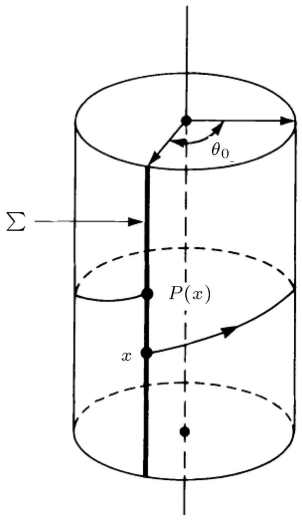

Figure 1. The Poincaré map of a first-order non-autonomous system [16].

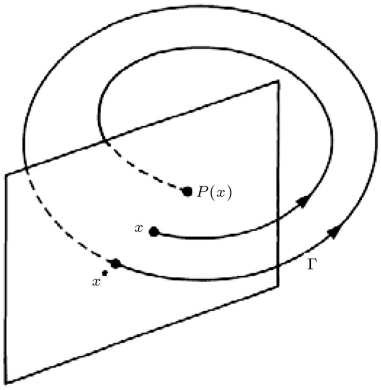

Figure 2. The Poincaré map of a third-order autonomous system [16].

P_N is called the Poincaré map of the non-autonomous system. Subscript N stands for non-autonomous and is used to distinguish this map from the Poincare maps that are used with autonomous systems.

The Poincaré map of autonomous systems: Consider an nth-order autonomous system with limit cycle Γ shown in Figure 2. Let x^* be a point on the limit cycle and let $\sum$ be an $(n-1)$-dimensional hyper plane transversal to T at x^*. The trajectory emanated from x^* will hit $\sum$ at x^* in T seconds, where T is the minimum period of the limit cycle. Due to the continuity of φ_t with respect to the initial condition, trajectories starting on $\sum$ in a sufficiently small neighborhood of x^* will, in approximately T seconds, intersect $\sum$ in the vicinity of x^*. Hence, φ_t and $\sum$ define a mapping PA of some neighborhood $U \subset \sum$ of x^* onto another neighborhood $V \subset \sum$ of x^*. PA is a Poincaré map of the autonomous system [16,17].

3. Materials and methods

3.1. Data

One of the main casualties in ASD children is the fact that they do not cooperate in recording, and that is why opened or even closed eye EEG recording is rarely talked about. In this research, with the close cooperation of Hedayate-noor autism center of Mashhad and Ibne-Sina Hospital and Aren center, not only are these casualties overcome, but also a new protocol based on common shapes of children's brain dynamics is presented.

In the present study, 60 ASD children (45 boys and 5 girls from 3 to 11 years old) and 60 normal children (50 boys and 10 girls from 3 to 11 years old) are chosen; having filled the EEG recording protocol form, they were diagnosed by an specialist based on DSM5 criteria.

Data, in this research, are recorded by ProComp5

Infiniti™ and EEG double channel recording on C3 and C4 electrodes with sampling frequency of 256 Hz. Data recording process consists of filling the questionnaire by parents and recording in a sound room with two channels (in C3 and C4 channels in 10-20 system). The child is first put in the sound room and EEG is recorded for 2 minutes. Then, his/her favorite animation is played for 5 minutes. Then, the same animation is played without sound, and the kid pays full attention to the screen in both cases.

Hence, in this process, there are three conditions in each case: base form (2 minutes), *watching the animation with audio* (V-A) for 5 minutes, and *watching the animation with muted audio band* (VwA) for 5 minutes. It is worth mentioning that sound room is an acoustic room without any environmental noises with precise sound and voice control for children empowerment in the center. C3 and C4 channels are used for two reasons: clinical and technical (Figure 3).

The primary reason is the fact that installation of the children from the middle of spectrum to the rest with recording cap using plate-like electrodes (made with gold and special jelly with temporary conductivity and adhesion) is easy and quick; moreover, C3 and C4 in 10-20 systems have the most stability even in case of head movement. The second reason is the former studies based on the importance of mirror and MU rhythm in ASD studies [10,18-24].

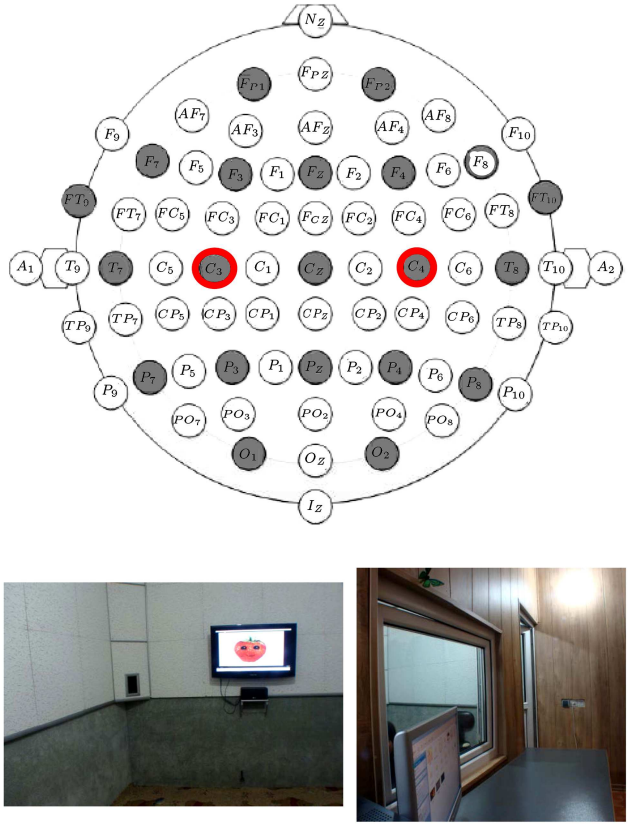

Figure 3. Location of electrodes in international 10-20 system; the used channels are shown with gray color and red line and sound room.

The core question of data recording is that CT and MRI are both advanced neuroimaging tools. Why do we still choose EEG in this research? Two main reasons are:

1. It is important to note that in the living system, global order or coherence must be sustained and maintained over time, so CT and MRI are not good choices for date recording for dynamical studies;
2. CT cannot represent adequate information even for statistical analysis, but fMRI is better. However, using fMRI is expensive and limited centers could follow up on it, so using EEG is a sine qua non for screening and investigating the studies.

3.2. Procedure

To extract information, instead of using methods based on signal amplitude, an independent method from amplitude and energy can be applied. In normal quantifications of QEEG, amplitude and signal energy in different bands are solely considered, but to obtain signal information, we have to look for transformations which take signal to information phase. In this research, Poincaré section is used for extracting information from signal and new indexes are also introduced for its quantification. In this section, first, we focus on how to implement Poincaré section on EEG signal, and then move on to the extracted features. In terms of optimum feature investigation, to compare the two groups of independent t-test, two channels in a group of paired t-test and two channels in two groups of Repeated Measures Analysis of Covariance are used; Pearson test is also used to investigate the relation between situations of with and without voice.

3.3. Poincaré section

Three general methods are used for Poincaré section: time sampling, sampling with regard to special events, and geometrical methods. Time sampling, known as stroboscopic, is mostly used in the study of autonomous systems with a single alternating input [25]. Stroboscopic is known as the origin of Poincaré section in which the vantage point is the geometrical intersection with trajectories regardless of the sampling time. Sampling with regard to special events mostly reveals the peaks, such as the interval between two heart beats. Geometrical section is a general method and does not have a special application. Based on Takens' theory, if time series of one of the outputs of a set of differential equations is available, by using it, phase plane with a dimension twice as much as the main phase state with the same basic features can be reconstructed [26]. These basic characteristics include dimension, Lyapunov exponents, and entropy [27]. The min idea in phase space reconstruction and study of

system's dynamics is to determine the present sample from the former, and time series follows a differential equation or a recursive transformation [28,29]. To reconstruct phase plane, knowing space dimension (m) and delay (τ) is essential; hence, these values have to be estimated [29]. Considerable point is the fact that there exists more than one method for this purpose; for instance, delay can be estimated with correlation dimension and mutual information [30]. To estimate the correlation dimension, Higuchi [31] and False Nearest Neighbor (FNN) can be used [32]. Auto-correlation or mutual information are defined with random signals, and they are used to estimate the state of dynamical signals that variables in each moment are generated from the previous moment, which is notable [33,34].

In addition, reconstructed phase plane is sensitive to delay and reconstruction dimension, while estimated values, using different methods, are considerably different. Moreover, most of the times, the estimated dimension is more than 3, and it is shown in 2 or 3 dimensions due to practical reasons [35,36]; in fact, the estimated reconstructed dimension is left useless [36].

Another considerable point is the fact that in the reconstructed space [37], the limits of all variables are the same as those of the used variable. In [38], EEG is presented in two dimensions with different reconstructing delays. Despite some initial assumptions in some papers, it is said that many chaotic systems (e.g., Lorenz, Russler), signals (i.e., EEG), and their phase plane reconstruction are not sensitive to (m) [39]. According to what was mentioned above, although most of the studies on phase plane reconstruction are considered as the foundation of theoretical problem solving, they do not implement it in practice. One of the approaches to phase space reconstruction is *relativism*, and this method is accompanied by a relative approach to the system. In this method, depending on the sampling frequency, each sample can be presented with regard to the previous one. What happens in Takens' theory phase plane reconstruction leads to such a presentation. However, two major differences of this method are:

1. The non-requirement of any delay and system dimension estimation;
2. Not claiming at all that this method is capable of achieving new variables and their representations.

In most of the resources, these diagrams are called Lorenz or Poincaré. But, the main difference of this method from Poincaré diagram is that the reconstructed diagram is not determined using this approach by Poincaré section [37,40]. After representation in the proper space, a proper section is to be determined. This step is of high importance, and numerous methods can be implemented for choosing a proper section which indeed is dependent on the application of cybernetic signal. If the goal is to determine system's dynamics, periodic or chaotic, Poincaré section is chosen correctly when it intersects all the trajectory rings [41]. In fact, in this series of problems, each intersection point is a representation of an orbit of the trajectory. If there is one point with the mentioned features, it is that the behavior is periodic one. In this approach, the working point of the system can be the intersecting point on the section (special state), or this trajectory will pass the same point. With an increase in the section points, system's period will be 2, 3, etc. Only the time sequence of the points can be determined using phase space and Poincaré section results, and no conclusion can be made with regard to the time distance between them [42]. In the relative representation of the two-dimensional space, line section (straight line or curve) is appropriate.

In our point of view, choosing the section determines the question which is asked of the system's dynamics, and the more technical the question is, the more perspectives of the dynamics it reveals. But, what is an appropriate section? The answer consists of two contradictory parts; a proper section has more intersection points and is placed where we have the most stretching of the signal. In fact, there should be a balance between the numbers of intersection point and stretching, which are like stability and flexibility of the system, or to make it more simple, like acceleration and brake. In the following, to choose the indexes, both above-mentioned points are considered simultaneously: one is known as number of point (HD) and one as divergence (D). In Figure 4, two-dimensional relative representation and first-order intersection with $y = \alpha x + \beta$ are used, and $\alpha = 1$, $\beta = 0$ [43]. In other words, the relation of the points on the section is in the form of $x_{n+1} = x_n$.

4. Feature extraction

The most important aspect in Poincaré section is the arrangement of the points on the section; in other words, the extracted information from Poincaré section is from the points. The important question here is the informative essence of Poincaré section, which is shown in Figure 5. As it can be clearly seen, using Poincaré section, point #1 which has a great difference in amplitude compared to point #3 is chosen as a section point, but point #2 that has a little difference compared to point #3 is not chosen; therefore, this is the informative approach that depletes energy.

In this research, divergence index is used to investigate the arrangement of the Poincaré section points. In this criterion, in this index, Euclidean distance of all points from the average point is used as an index. As shown in Figure 6, suppose n

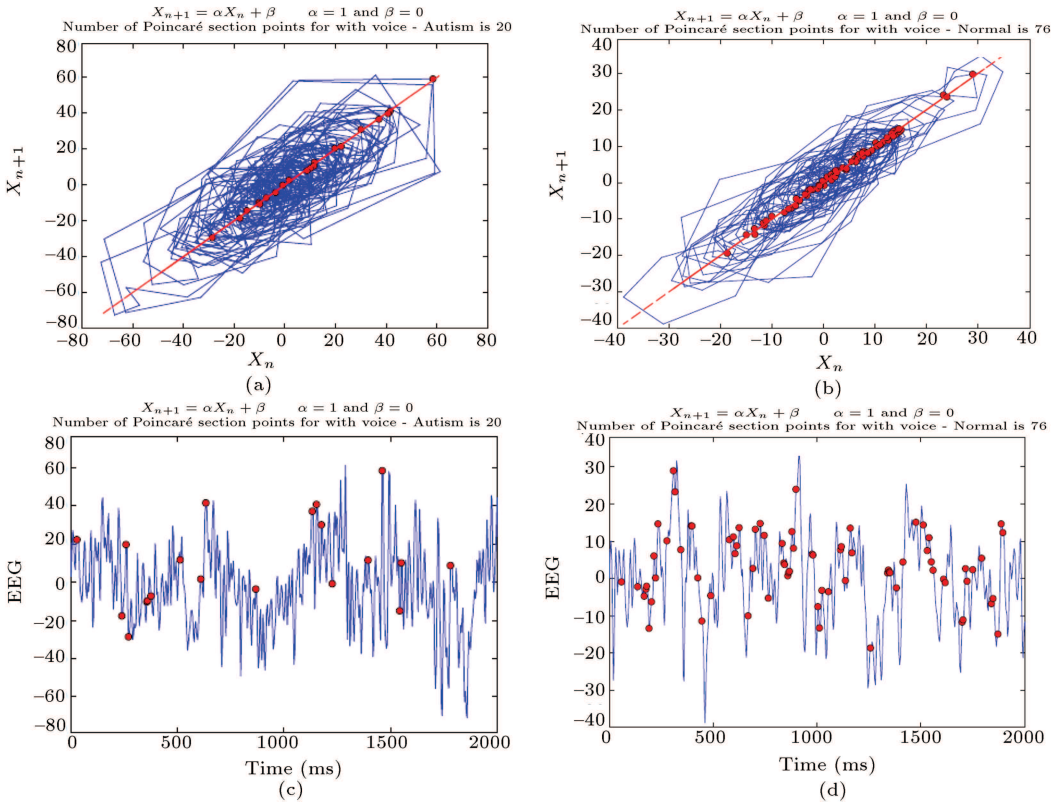

Figure 4. Poincaré section of EEG signal in relativistic reconstructed phase plane ((a) and (b)) and time domain ((c) and (d)) with $Y = X$ section and the same length. (a) and (c) is Autism in V-A and (b) and (d) are normal.

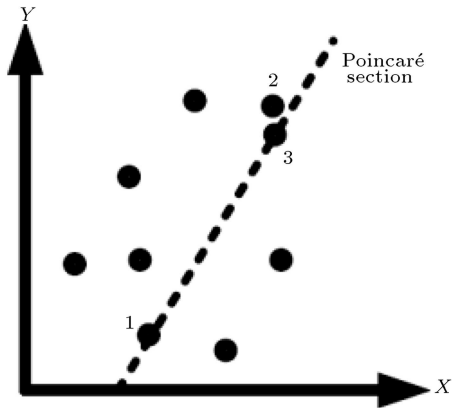

Figure 5. Informative essence of Poincaré.

points of Poincaré section in two-dimensional space. These points are arranged as n columns of matrix $\mathbf{P}$ ($\mathbf{P} \in \Re^{2\times N}$) and $\mathbf{P} = [p_1, p_2, \cdots, p_N]$. Average of all points in vertical and horizontal angles is p_m ($p_m \in \Re^2$) and yields $p_m = \frac{1}{n}\sum_{i=1}^{N} p_i$; then, the sum of Euclidean distances between p_i and p_m is computed from Eq. (6) [44], meaning Euclidean norm and Heaviside function presented in Eq. (7):

$$d_i = \|p_i - p_m\|, \tag{6}$$

$$\%endgather\Theta(x) = \begin{cases} 0 & x < 0 \\ 1 & x \geq 0 \end{cases} \tag{7}$$

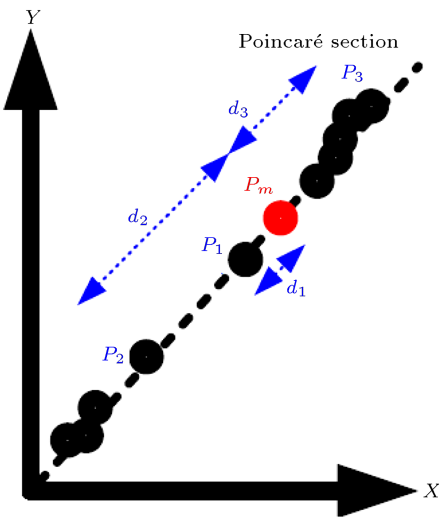

Figure 6. Index for ordering of point in Poincaré section.

$$\text{Div} = \sum_{i=1}^{N} d_m, \tag{8}$$

$$\text{HD} = \sum_{i=1}^{N} \Theta(Hthr - d_i), \tag{9}$$

$$C(R) = \frac{1}{N-1}\sum_{i=1}^{N}\sum_{j=1, j\neq i}^{N} \Theta(x_i - x_j). \tag{10}$$

The extracted features in this state investigate the arrangement of the Poincaré points with regard to the dispersion. Different features were extracted from the Poincaré section from which two are labeled as "*important*":

1. Number of Poincaré points whose distance from the center of gravity is higher than the threshold ($d_m > Hthr$) as in Eq. (9). This concept resembles correlation sum, yet with considerable difference; having a definite direction on trajectory that can also be named "Poincaré Section". The parameter "HD", introduced in Eq. (9), focuses on definite direction while C(R), in Eq. (10), is about definite distance;
2. The overall dispersion calculated from Eq. (8) that is synonymous with stretching-folding concept. In the following, we work on statistical analysis of the results and their features.

5. Results

Based on the two features already mentioned, we are going to analyze each index in the following. HD Index: As already mentioned, this feature shows the number of points from Poincaré section (in each 4 seconds) whose distance from intersection points' weight point (P_m in the above figure) is more than the threshold ($d_m > Hthr$). In other words, this feature investigates the divergence of the Poincaré section points. HD index in two channels C3 and C4 in VwA and V-A situations is investigated. Figure 7 shows four recent features.

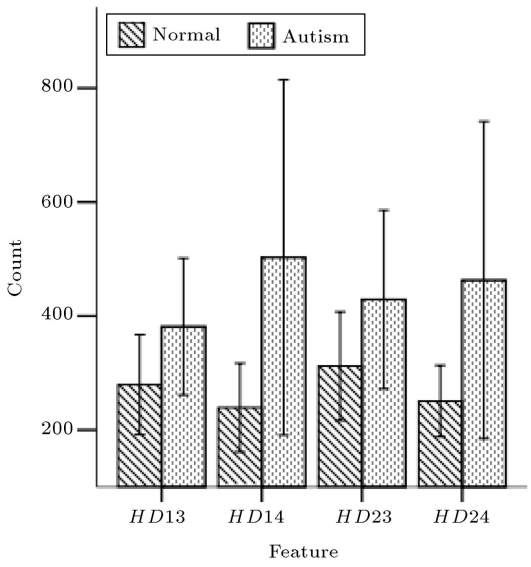

Figure 7. Comparison of HD index in normal and ASD cases. Dxx definition: xx is 13 with VwA situation and C3 electrode; is 14 with VwA situation and C4 electrode; is 23 with V-A situation and C3 electrode; and is 24 with V-A situation and C4 electrode.

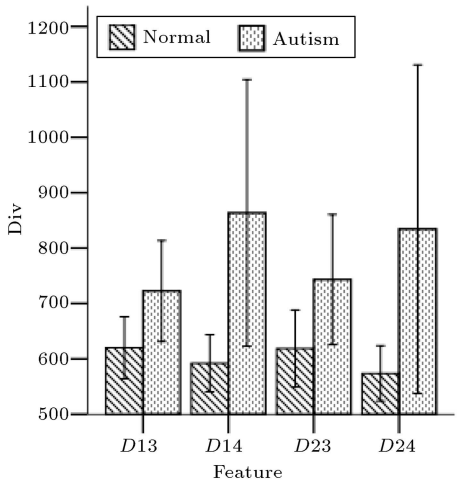

Figure 8. Comparison of D index in normal and ASD cases. HDxx definition: xx is 13 with VwA situation and C3 electrode; is 14 with VwA situation and C4 electrode; is 23 with V-A situation and C3 electrode; and is 24 with V-A situation and C4 electrode.

As shown in Figure 7, a distinctive difference is observable between the normal and ASD cases in HD criteria under both VwA and V-A situations; the intensified difference in VwA situation is also an interesting fact.

D Index shows the value of *Div* outcome of Eq. (8) and demonstrates the general divergence; smaller number means more folding and larger number means more stretching.

As can be seen (in Figure 8), divergence in ASD case is much more than normal cases. The second point is that asymmetry in hemispheres, the region in which 95% of the data lie, is much smaller in normal cases compared to ASD, and this difference maximizes C4 electrode. To investigate the optimum index and to compare two groups of independent t-test, two channels in a group paired t-test and two channels in two groups of Repeated Measure analysis of covariance are used. Pearson test is also used to investigate the relation between VwA and V-A with and without situations; all statistical analyses are done with PASWStatistics18@. In Table 2, the Null hypothesis is: Holistic features D14 (VwA state on channel C4) and HD24 (V-A state on channel C4) cannot discriminate normal cases from ASD ones. Alternative hypothesis states that D14 and HD24 can discriminate normal cases from ASD ones. Then, the null hypothesis is rejected in favor of the alternative hypothesis ($P < 0.05$). The comparison between normal and ASD groups is done using independent t-test; considerable difference is observable in D index on C4 in VwA situation, $t(120) = 6.582$, $P = 0.01$, and in HD on C4 in VwA situation, $t(120) = -1.546$, $P = 0.04$, (Table 2).

In Table 3, null hypothesis is that in normal children case, there is no hemispheric effect on the

Table 2. Results of independent t-test between ASD and normal children.

Feature	Normal	ASD	Statistical analysis	
	Mean (std)	Mean (std)	P	T-ratio
D14	592.155 (116.26)	863.39 (543.16)	0.01*	–2.29
HD24	250.68 (141.34)	462.9 (628.17)	0.04*	–1.54

Dxx or HDxx definition: xx is 13 with VwA situation and C3 electrode; is 14 with VwA situation and C4 electrode; is 23 with V-A situation and C3 electrode; and is 24 with V-A situation and C4 electrode.

*: $P < 0.05$

holistic features D and HD (in both VwA and V-A states). Alternative hypothesis is that in normal children case, there is significant hemispheric effect on the holistic feature D (in both VwA and V-A states). Then, the null hypothesis is rejected in favor of the alternative hypothesis ($P < 0.05$).

Table 3 shows the results of the comparison concerning hemispheric effect on a group using paired t-test with the aim of investigating the features on C3 and C4 channels.

Correlation test between D and HD indexes resulted from different recording channels; audio measure is shown in Table 4:

1. D and HD indexes in normal and ASD cases are greatly dependent on audio (Table 3), while this dependence in normal case is more considerable in comparison with ASD cases;
2. In the situation of muted audio band (VwA), HD index is related to the channel in normal cases, while it is not in ASD cases; hence, HD1 index is able to show the effect of ASD on asymmetry and brain functionality;
3. In the situation of watching animation with audio (V-A), HD index is dependent on the channel in both cases;
4. In the situation of 'without sound', D index is dependent on channel, but it is not in ASD cases; hence, D1 index is able to show the effect of ASD on asymmetry and brain functionality;
5. In the situation of watching animation with audio (V-A), D index is dependent on the channel in both cases.

Table 3. Paired t-test for ASD and normal for hemispheric effect.

Feature	ASD		Normal	
	T-ratio	P	T-ratio	P
D2	–0.928	0.363	2.5	0.02*
D1	–1.262	0.22	3.797	0.001**
HD1	–0.819	0.42	4.45	2.16E-4***
HD2	–0.47	0.642	2.65	0.014*

Dxx or HDxx definition: xx is 13 with VwA situation and C3 electrode; is 14 with VwA situation and C4 electrode; is 23 with V-A situation and C3 electrode; and is 24 with V-A situation and C4 electrode.

*: $P < 0.05$, **: $P < 0.005$, ***: $P < 0.0005$

6. Conclusion

Early identification of Autism Spectrum Disorder (ASD) is essential to ensure that children can access specialized evidence-based interventions that can help to optimize long-term outcomes [45]. Poincaré section is a holistic approach based on information and cybernetics concepts that could help us for early

Table 4. Effect of situation and electrode position on features in ASD and normal children.

Feature × situation	Normal		ASD	
	$P(N)$	Pearson coefficient	P(ASD)	Pearson coefficient
HD ×voice	2E-7	0.865	0.01	0.49
D ×voice	3.5E-8	0.88	0.01	0.528
HD1 ×electrode	7.85E-16*	0.98	0.318	0.22
HD2 ×electrode	1.82E-8	0.895	3.84E-9	0.911
D1 ×electrode	7.18E-13*	0.963	0.20	0.282
D2 ×electrode	3.22E-7	0.85	2.43E-7	0.862

Dxx or HDxx definition: xx is 13 with VwA situation and C3 electrode; is 14 with VwA situation and C4 electrode; is 23 with V-A situation and C3 electrode; and is 24 with V-A situation and C4 electrode.

*: P(ASD) < 0.0005 and $P(N) > 0.25$

identification of ASD. In this research, two criteria, including divergence size (D) with inspiration from signal stretching-folding and number of intersection points with more distance from the threshold (HD) with inspiration from correlation dimension, are extracted from the analyses.

Distinctive difference is observable in counts and variations of HD and D criteria between the normal and ASD cases in VwA, because ASD children have abnormal cortical voice processing [46], and we have significant difference in D index on C4 in VwA situation ($t(120) = 6.582$, $P = 0.01$) and in HD on C4 in VwA situation ($t(120) = -1.546$, $P = 0.04$). Paired t-tests of HD13 and HD14 of ASD and normal cases show highly significant difference in HD1 index (DH in VwA situation) in C3 and C4 electrodes, indicating that the number of intersection points with more distance from threshold (HD) in left (C3) and right (C4) hemispheres in normal cases (as opposed to ASD cases) has significant difference ($P < 0.0005$). In other words, hemispheric asymmetry in ASD children does not follow normal patterns, so in terms of the hemispheric asymmetry, D and HD are very effective biomarkers that make a distinction between ASD and normal cases. Our approach is based on this fact that the dynamic balance among interactions of different basin of attractions is synonymous to self-organization in basin of healthy.

7. Future directions

Development on ASD biomarkers could lead to early detection or even screening and investigation in the studies. Two essential features are: data recording protocol of ASD children and detection of episodic patterns (complexes) as hallmark of ASD dynamic. Arrangement as an empirical measure of nonrandom complexity could detect these complexes. Together, these enabling technologies and new models will likely push the field forward significantly in the next few years.

References

1. Sabelli, H., Lawandow, A. and Kopra, A. "Asymmetry, symmetry and beauty", *Symmetry*, **2**(3), p. 1591 (2010).
2. Enquist, M. and Arak, A. "Symmetry, beauty and evolution", *Nature*, **372**(6502), pp. 169-172 (1994).
3. Rogers, L.J., Vallortigara, G. and Andrew, R.J., *Divided Brains: The Biology and Behaviour of Brain Asymmetries*, Cambridge University Press (2013).
4. Association, A.P., *Diagnostic and Statistical Manual of Mental Disorders (DSM-5®)*, American Psychiatric Pub. (2013).
5. Patterson, P.H. "Modeling autistic features in animals", *Pediatr Res.*, **69**(5, Part 2 of 2), pp. 34R-40R (2011).
6. Sadeghi Bajestani, G., Sheikhani, A., Hashemi Golpayegani, S.M.R., Ashrafzadeh, F. and Hebrani, P. "A systematic review, on the application of quantitative EEG for characterizing autistic brain", *Modern Rehabilitation*, **9**(6), pp. 10-28 (2016).
7. Owen-Smith, A.A., Bent, S., Lynch, F.L., Coleman, K.J., Yau, V.M., Pearson, K.A., Massolo, M.L., Quinn, V. and Croen, L.A. "Prevalence and predictors of complementary and alternative medicine use in a large insured sample of children with autism spectrum disorders", *Research in Autism Spectrum Disorders*, **17**, pp. 40-51 (2015).
8. Lazarev, V., Pontes, A. and Mitrofanov, A. "Interhemispheric asymmetry in EEG photic driving coherence in childhood autism", *Clinical Neurophysiology*, **121**(2), pp. 145-152 (2010).
9. Ogawa, T., Sugiyama, A., Ishiwa, S., Suzuki, M., Ishihara, T. and Sato, K. "Ontogenic development of EEG-asymmetry in early infantile autism", *Brain and Development*, **4**(6), pp. 439-449 (1982).
10. Strzelecka, J. "Electroencephalographic studies in children with autism spectrum disorders", *Research in Autism Spectrum Disorders*, **8**(3), pp. 317-323 (2014).
11. Hirai, M., Gunji, A., Inoue, Y., Kita, Y., Hayashi, T., Nishimaki, K., Nakamura, M., Kakigi, R. and Inagaki, M. "Differential electrophysiological responses to biological motion in children and adults with and without autism spectrum disorders", *Research in Autism Spectrum Disorders*, **8**(12), pp. 1623-1634 (2014).
12. Lapenta, O.M. and Boggio, P.S. "Motor network activation during human action observation and imagery: Mu rhythm EEG evidence on typical and atypical neurodevelopment", *Research in Autism Spectrum Disorders*, **8**(7), pp. 759-766 (2014).
13. Rutter, M.L. "Progress in understanding autism: 2007-2010", *Journal of Autism and Developmental Disorders*, **41**(4), pp. 395-404 (2011).
14. Golnik, A.E. and Ireland, M. "Complementary alternative medicine for children with autism: A physician survey", *Journal of Autism and Developmental Disorders*, **39**(7), pp. 996-1005 (2009).
15. Griffin, R. and Westbury, C. "Infant EEG activity as a biomarker for autism: a promising approach or a false promise?", *BMC Medicine*, **9**(1), p. 61 (2011).
16. Parker, T.S. and Chua, L., *Practical Numerical Algorithms for Chaotic Systems*, Springer Science & Business Media (2012).
17. Hilborn, R.C. "Chaos and nonlinear dynamics: an introduction for scientists and engineers", *Computers in Physics*, **8**(6), pp. 689-689 (1994).
18. Dumas, G., Soussignan, R., Hugueville, L., Martinerie, J. and Nadel, J. "Revisiting mu suppression in autism spectrum disorder", *Brain Research*, **1585**, pp. 108-119 (2014).

19. Bernier, R., Dawson, G., Webb, S. and Murias, M. "EEG mu rhythm and imitation impairments in individuals with autism spectrum disorder", *Brain and Cognition*, **64**(3), pp. 228-237 (2007).

20. Friedrich, E.V., Suttie, N., Sivanathan, A., Lim, T., Louchart, S. and Pineda, J.A. "Brain-computer interface game applications for combined neurofeedback and biofeedback treatment for children on the autism spectrum", *Frontiers in Neuroengineering*, **7**, p. 21 (2014).

21. Khan, S., Michmizos, K., Tommerdahl, M., Ganesan, S., Kitzbichler, M.G., Zetino, M., Garel, K.L.A., Herbert, M.R., Hämäläinen, M.S. and Kenet, T. "Somatosensory cortex functional connectivity abnormalities in autism show opposite trends, depending on direction and spatial scale", *Brain*, **138**(5), pp. 1394-1409 (2015).

22. Cuevas, K., Cannon, E.N., Yoo, K. and Fox, N.A. "The infant EEG mu rhythm: Methodological considerations and best practices", *Developmental Review*, **34**(1), pp. 26-43 (2014).

23. Coll, M.P., Bird, G., Catmur, C. and Press, C. "Cross-modal repetition effects in the mu rhythm indicate tactile mirroring during action observation", *Cortex*, **63**, pp. 121-131 (2015).

24. Brown, E.C., Gonzalez-Liencres, C., Tas, C. and Brüne, M. "Reward modulates the mirror neuron system in schizophrenia: A study into the mu rhythm suppression, empathy, and mental state attribution", *Social Neuroscience*, pp. 1-12 (2015).

25. Denton, T.A. and Diamond, G.A. "Can the analytic techniques of nonlinear dynamics distinguish periodic, random and chaotic signals?", *Computers in Biology and Medicine*, **21**(4), pp. 243-263 (1991).

26. Stam, C.J. "Nonlinear dynamical analysis of EEG and MEG:Review of an emerging field", *Clinical Neurophysiology*, **116**, pp. 2266-2301 (2005).

27. Takens, F. "Detecting strange attractors in turbulence", *Lecture Notes in Mathematics*, **898**, pp. 366-381 (1981).

28. Liu, Z. "Chaotic time series analysis", *Mathematical Problems in Engineering*, **2010**, p. 31 (2010).

29. Takens, F. "Detecting strange attractors in turbulence", *Lecture Notes in Mathematics*, **898**(1), pp. 366-381 (1981).

30. Andrew, M.F. and Swinney H.L. "Independent coordinates for strange attractors from mutual information", *Phys. Rev. A 33, 1134*, **33**(2), pp. 1134-1140 (1986).

31. Higuchi, T. "Approach to an irregular time series on the basis of the fractal theory", *Physica D: Nonlinear Phenomena*, **31**(2), pp. 277-283 (1988).

32. Hegger, R. and Kantz, H. "Improved false nearest neighbor method to detect determinism in time series data", *Physical Review E*, **60**(4), p. 4970 (1999).

33. Grassberger, P. "Generalized dimensions of strange atfractors", *Physics Letters A*, **97**(6), pp. 227-230 (5 Sept. 1983).

34. Kennel, M.B., Brown, R. and Abarbanel, H.D.I. "Determining embedding dimension for phase-space reconstruction using a geometrical construction", *Phys. Rev. A, 3403 - Published*, **45**(6), pp. 3403-3411 (1 March 1992).

35. Dvorak, I. and Siska, J. "On some problems encountered in the estimation of the correlation dimension of the EEG", *Physics Letters A*, **118**(2), pp. 63-66 (Sept. 1986).

36. Dvořák, I. "Takens versus multichannel reconstruction in EEG correlation exponent estimates", *Physics Letters A*, **151**(5), pp. 225-233 (10 Dec. 1990).

37. Sharma, R. and Pachori, R.B. "Classification of epileptic seizures in EEG signals based on phase space representation of intrinsic mode functions", *Expert Systems with Applications*, **42**(3), pp. 1106-1117 (15 Feb. 2015).

38. Jianbo, G., Hu, J. and Tung, W. "Complexity measures of brain wave dynamics", *Cognitive Neurodynamics*, **5**(2), pp. 171-182 (2011).

39. Rong-Yi, Y. and Xiao-Jing, H. "Phase space reconstruction of chaotic dynamical system based on wavelet decomposition", *Chinese Physics B*, **20**(2), p. 020505 (2011).

40. Dabanloo, N.J., Moharreri, S., Parvaneh, S. and Nasrabadi, A.M. "Application of novel mapping for heart rate phase space and its role in cardiac arrhythmia diagnosis", In *Computing in Cardiology*, **2010**, pp. 209-212 (2010).

41. Hilborn, R., *Chaos and Nonlinear Dynamics: An Introduction for Scientists and Engineers*, USA: Oxford University Press (Jan. 11, 2001).

42. Piskorski, J. and Guzik, P. "Geometry of the Poincaré plot of RR intervals and its asymmetry in healthy adults", *Physiological Measurement*, **28** (IOP Publishing), pp. 287-300 (2007).

43. Bajestani, G.S., Sheikhani A., Hashemi Golpayegani, M.R., Ashrafzadehi, F. and Hebrani, P. "Cybernetic approach in identification of brain pattern variations in autism spectrum disorder. Biomedical Engineering: Applications", *Basis and Communications*, **28**(01), p. 1650006 (2016).

44. Jafari, S., Sprott, J.C., Pham, V., Hashemi Golpayegani, S.M.R. and Jafari, A.H. "A new cost function for parameter estimation of chaotic systems using return maps as fingerprints", *International Journal of Bifurcation and Chaos*, **24**(10), p. 1450134 (2014).

45. Woods, J.J. and Wetherby, A.M. "Early identification of autism spectrum disorder: Recommendations for practice and research", *Pediatrics*, **136**(Supplement 1), pp. S10-S40 (2015).

46. Gervais, H., Belin, P., Boddaert, N., Leboyer, M., Coez, A., Sfaello, I., Barth'el'emy, C., Brunelle, F., Samson, Y. and Zilbovicius, M. "Abnormal cortical voice processing in autism", *Nature Neuroscience*, **7**(8), pp. 801-802 (2004).

47. Okazaki, R., Takahashi, T., Koichi Takahashi, K., Ishitobi, M., Kikuchi, M., Higashima, M. and Wada, Y. "Changes in EEG complexity with electroconvulsive therapy in a patient with autism spectrum disorders: A multiscale entropy approach", *Frontiers in Human Neuroscience*, **9**, p. 106 (2015).

48. Hoole, P.R.P., Pirapaharan, K., Basar, S.A., Ismail, R., Liyanage, D.L.D.A., Senanayake, S.S.H.M.U.L. and Hoole S.R.H. "Autism, EEG and brain electromagnetics research" in *Biomedical Engineering and Sciences (IECBES), IEEE EMBS Conference on*, (2012).

49. Ahmadlou, M., Adeli, H. and Adeli, A. "Fractality and a wavelet-chaos-neural network methodology for EEG-based diagnosis of autistic spectrum disorder", *Journal of Clinical Neurophysiology*, **27**(5), pp. 328-333 (2010).

50. Duffy, F.H. and Als, H. "A stable pattern of EEG spectral coherence distinguishes children with autism from neuro-typical controls-a large case control study", *BMC Medicine*, **10**(1), p. 64 (2012).

51. Peters, J.M., Taquet, M. , Vega, C. , Jeste, S.S., Sánchez Fernández, I. , Tan, J., Nelson, C. A., Sahin, M. and Warfield, S.K. "Brain functional networks in syndromic and non-syndromic autism: a graph theoretical study of EEG connectivity", *BMC Medicine*, **11**(1), p. 54 (2013).

52. Goh, S., Dong, Z., Zhang, Y., DiMauro, S. and Peterson B.S. "Mitochondrial dysfunction as a neurobiological subtype of autism spectrum disorder: Evidence from brain imaging", *JAMA Psychiatry*, **71**(6), pp. 665-671 (2014).

53. Léveillé, C., Barbeau, E.B., Bolduc, C., Limoges, É., Berthiaume, C., Chevrier, É., Mottron, L. and Godbout, R. "Enhanced connectivity between visual cortex and other regions of the brain in autism: a REM sleep EEG coherence study", *Autism Research*, **3**(5), pp. 280-285 (2010).

54. Lazarev, V.V., Pontes, A. and Mitrofanov, A.A. "Interhemispheric asymmetry in EEG photic driving coherence in childhood autism", *Clinical Neurophysiology*, **121**(2), pp. 145-152 (2010).

55. Tierney, A.L., Gabard-Durnam, L., Vogel-Farley, V., Tager-Flusberg, H. and Nelson, C.A. "Developmental trajectories of resting EEG power: an endophenotype of autism spectrum disorder", *PloS One*, **7**(6), p. e39127 (2012).

56. Tierney, A.L., Gabard-Durnam, L., Vogel-Farley, V., Tager-Flusberg, H. and Nelson, C.A. *Developmental Trajectories of Resting EEG Power: An Endophenotype of Autism Spectrum Disorder*, Clinical Neurophysiology, **123**(9), pp. 1798-1809 (2012).

57. Mathewson, K.J., Jetha, M.K., Drmic, I.E., Bryson, S.E., Goldberg, J.O. and Schmidt, L.A. "Regional EEG alpha power, coherence, and behavioral symptomatology in autism spectrum disorder", *Clinical Neurophysiology*, **123**(9), pp. 1798-1809 (2012).

58. Coben, R., et al. "EEG power and coherence in autistic spectrum disorder", *Clinical Neurophysiology*, **119**(5), pp. 1002-1009 (2008).

59. Isler, J.R., et al. "Reduced functional connectivity in visual evoked potentials in children with autism spectrum disorder", *Clinical Neurophysiology*, **121**(12), pp. 2035-2043 (2010).

60. Ahmadlou, M., Adeli, H. and Adeli, A. "Fuzzy synchronization likelihood-wavelet methodology for diagnosis of autism spectrum disorder", *Journal of Neuroscience Methods*, **211**(2), pp. 203-209 (2012).

61. Yasuhara, A. "Correlation between EEG abnormalities and symptoms of autism spectrum disorder (ASD)", *Brain and Development*, **32**(10), pp. 791-798 (2010).

Biographies

Ghasem Sadeghi Bajestani is a PhD student of Biomedical Engineering. His research interests are chaotic dynamics and applications, complexity theory and cybernetics.

Ali Sheikhani is an Assistant Professor of Biomedical Engineering, Islamic Azad University, Science and Research Branch, Tehran, Iran. His research interests are biomedical signal processing, signal processing, and bio instruments.

Seyed Mohammad Reza Hashemi Golpayegani is a Professor of Biomedical Engineering, Amirkabir University of Technology. His research interests are chaotic dynamics and applications, complexity theory and cybernetics.

Farah Ashrafzadeh is a Professor of Pediatric neurology, Mashhad University of Medical Sciences (MUMS) Mashhad, Iran. Her research interests are herbal therapy in epilepsy and Brain structural abnormality-Developmental delay.

Paria Hebrani is an Associate Professor of Child and Adolescent Psychiatry, Mashhad University of Medical Sciences (MUMS) Mashhad, Iran. Her research interests are ADHD, Autism.